Intensity and Polarization for Single Scattering by Polydisperse Spheres: A Comparison of Ray Optics and Mie Theory

KUO-NAN LIOU AND JAMES E. HANSEN

Goddard Institute for Space Studies, NASA, New York, N. Y.

(Manuscript received 16 March 1971)

ABSTRACT

The intensity and polarization for single scattering by large spherical particles are computed using both the exact Mie theory and the approximation of ray optics. It is found that the ray-tracing method can yield accurate results for particle size parameters in the range of interest for some meteorological applications, where the size parameter is the ratio of the particle circumference to the wavelength of the incident light. Since this method is practical for application to nonspherical particles, it should be of use in studies of cloud microstructure. The ray-optics method is also useful in the case of spherical particles because it provides a physical explanation for features which occur in the exact theory.

The ray-optics calculations include Fraunhofer diffraction as well as geometrical reflection and refraction; rays undergoing one or two internal reflections, which give rise to the observable rainbows, are also included. Calculations are made for non-absorbing and absorbing spheres for several refractive indices in the range $1.1 \leqslant n_r \leqslant 2.0$. Comparisons between the ray-optics approximation and the exact Mie theory are made for $n_r = 1.33$ and 1.50. It is found that the two methods are in close agreement, if the particle size parameter is $\gtrsim 400$. It is also shown that, to a good approximation, the ray-optics solution may often be used to obtain the entire phase matrix for single scattering.

1. Introduction

The laws of geometrical optics may be used to compute the angular distribution of light which is scattered when a plane electromagnetic wave is incident on a particle much larger than the wavelength of the incident light. Such a computation is an approximation based on the assumption that the light may be thought of as consisting of separate *localized* rays which travel along straight line paths; it is an asymptotic approach which becomes increasingly accurate in the limit as the size/wavelength ratio approaches infinity. In this paper we use the terminology *geometrical optics* to include rays externally reflected by the particle and rays refracted into the particle; the latter rays may be absorbed in the particle or they may emerge from it after possibly suffering some internal reflections. The total energy scattered and absorbed by the particle in geometrical optics is hence equal to that impinging on the cross section of the particle presented to the incident beam.

Particles much larger than the wavelength also scatter light by the phenomenon of diffraction, which removes energy from the light wave *passing by* the particle. The diffraction is concentrated in a narrow lobe around the forward direction, and, like geometrical reflection and refraction, it contains an amount of energy equal to that incident on the particle's cross section. In the far field, i.e., at a distance much greater than the particle size, this diffracted component of the scattered light may be approximated by Fraunhofer diffraction theory. The diffraction depends only on the shape of the particle's cross section, i.e., its shadow, and the ratio of the shadow size to the incident wavelength; for spherical particles it hence depends only on the size parameter, $x = 2\pi r/\lambda$. In this paper, for convenience, we refer to *ray optics* as including geometrical reflection and refraction plus Fraunhofer diffraction. In our computations we add these different contributions without regard to phase; this is reasonable since we are interested in results for polydispersions for which phase effects would largely be washed out.

Geometrical optics has been used extensively, e.g., by van de Hulst (1957), Shifrin (1951), Shifrin and Rabinowitz (1957) and Volz (1961), to calculate light scattering from a spherical water drop in order to help understand the scattering pattern including the rainbow features. Hodkinson and Greenleaves (1963) have used ray optics to calculate scattered intensities for spherical particles with scattering angles up to $\sim 40°$; they included comparisons to Mie theory, although the size parameter for the Mie computations did not exceed 30. Recently a ray-optics approach has also been used for non-spherical particles by Jacobowitz (1970), who calculated the angular scattering pattern for hexagonal ice crystals.

Since the application of ray optics to finite particles is an approximation, it is important to obtain quantita-

tive information on the size parameter limits within which the method can be used to a given degree of confidence. The primary purpose of this paper is to obtain such information by comparing Mie scattering calculations for large spheres to calculations for ray optics. The results also help provide an understanding of features which occur in the intensity and polarization of light scattered by spheres. The Mie scattering results are obtained for a size distribution of spheres in order that the numerous interference maxima and minima, which occur for a single sphere, are smoothed out; this allows a fair comparison to be made to the results for ray optics. The computations in this paper are made primarily for refractive indices of 1.33 and 1.50, which are indices of special interest for applications to the terrestrial atmosphere.

2. Ray optics

In this section we describe the method used for the ray-optics computations with a polydispersion of spheres. Most of the notation is the same as that used by van de Hulst (1957) who gave detailed results for a sphere having a real refractive index $n_r=\frac{4}{3}$ in the special case of no absorption ($n_i=0$, where n_i is the imaginary part of the refractive index n).

For a single sphere the different contributions to the scattered intensity (the diffraction, reflection, and refraction with and without internal reflection) optically interfere, due to phase differences for these different contributions. This gives rise, in the case of large particles, to rapidly oscillating intensities as a function of scattering angle. However, if the particles are randomly located and separated by distances much larger than the incident wavelength, the intensities from the separate particles may be added without regard to phase; for a polydispersion of such particles the numerous maxima and minima are then lost in the integration over particle size. In the case of ray optics for a polydispersion it is hence reasonable to ignore the phase altogether in adding the intensities for diffraction, reflection and refraction. This simplifies the computations significantly.

We define the gain G, which gives a relative scattered intensity as a function of scattering angle, such that the average gain over the entire solid angle 4π is equal to $\tilde{\omega}_0$, the albedo for single scattering, i.e., the ratio of the scattered energy to that scattered and absorbed. The gain is thus the ratio of the scattered intensity to that which would exist if the radiation were scattered isotropically and conservatively, and may be expressed for ray optics as

$$G_{1,2}=G^F_{1,2}+\sum_{p=0}^{N} G^{(p)}_{1,2}. \tag{1}$$

The subscripts 1 and 2 refer to intensity components perpendicular and parallel, respectively, to the scattering plane; the notation is meant to indicate that Eq. (1) represents two equations, one for each polarization component. $G^F_{1,2}$ is the contribution of Fraunhofer diffraction to the gain and is the same for both polarization components, while $G^{(p)}_{1,2}$ is the contribution to the gain from geometrical optics, which includes external reflection ($p=0$), refraction ($p=1$), and internal reflection ($p\geq 2$). The value of N should theoretically be infinity, but in practice a small integer is sufficient; for most refractive indices $N=3$, which includes as many as two internal reflections, is sufficient to account for more than 99% of the scattered energy.

a. Geometrical optics

The contribution $G^{(p)}_{1,2}$ may be obtained from the laws of geometrical optics for each value of p by making computations for many values of the incident direction τ in the full range 0–90°. This direction is measured with respect to the surface of the particle; it is 90° for central incidence and 0° for grazing incidence. The scattering angle, $\theta(\tau)$, is computed individually for each value of p. The part of the incident ray refracted into the sphere ($p\geq 1$) enters at an angle τ' given by Snell's law, $n_r\cos\tau'=\cos\tau$. Since we are neglecting the phase, the gain for geometrical optics may be expressed as

$$G^{(p)}_{1\,2}(\theta,x)=2\epsilon^2_{1,2}D\exp(-4xn_ip\sin\tau') \tag{2}$$

where

$$\epsilon^2_{1,2}=\begin{cases}|r_{1,2}|^2, & \text{for } p=0,\\ (1-|r_{1,2}|^2)^2(|r_{1,2}|^2)^{p-1}, & \text{for } p\geq 1,\end{cases} \tag{3}$$

$r_{1,2}$ are the Fresnel reflection coefficients given by Born and Wolf (1962), i.e.,

$$\left.\begin{aligned} r_1&=\frac{\sin\tau-n\sin\tau'}{\sin\tau+n\sin\tau'}\\ r_2&=\frac{n\sin\tau-\sin\tau'}{n\sin\tau+\sin\tau'}\end{aligned}\right\}, \tag{4}$$

and x is the size parameter. The exponential in (2) accounts for absorption within the sphere; in the case of a non-absorbing sphere ($n_i=0$) the gain due to geometrical optics is independent of the particle size. The divergence D is given by

$$\left.\begin{aligned} D&=\frac{\sin\tau\cos\tau}{\sin\theta\,|d\theta/d\tau|}\\ \frac{d\theta}{d\tau}&=2-2p\frac{\tan\tau}{\tan\tau'}\end{aligned}\right\}. \tag{5}$$

The divergence arises because the incident ray is reflected and/or refracted by a curved surface. Eq. (5)

holds for spheres; it indicates that the divergence, and hence the intensity, becomes infinite in two special cases, both discussed in detail by van de Hulst (1957). The case $d\theta/d\tau=0$ gives rise to the well-known rainbow rays, while the case $\sin\theta=0$ with $\sin 2\tau\neq 0$ gives rise to infinite intensities for direct backscattering (the "glory") or direct forward scattering. In nature, infinite intensities do not occur, if for no other reason than the finite size of scatterers; however, the results for geometrical optics may still be accurate in the vicinity of the rainbow and glory angles.

The coefficients r_1 and r_2 are, in general, complex and hence the expressions for $|r_1|^2$ and $|r_2|^2$ are rather complicated. Following the procedure of Born and Wolf (1962, p. 627), we obtain

$$\left.\begin{aligned} |r_1|^2&=\frac{(\sin\tau-u)^2+v^2}{(\sin\tau+u)^2+v^2}\\ |r_2|^2&=\frac{[(n_r^2-n_i^2)\sin\tau-u]^2+(2n_rn_i\sin\tau-v)^2}{[(n_r^2-n_i^2)\sin\tau+u]^2+(2n_rn_i\sin\tau+v)^2}\end{aligned}\right\}, \tag{6}$$

where

$$\left.\begin{aligned} u&=\tfrac{1}{2}\{n_r^2-n_i^2-\cos^2\tau\\ &\qquad+[(n_r^2-n_i^2-\cos^2\tau)^2+4n_r^2n_i^2]^{\frac{1}{2}}\}\\ v&=\tfrac{1}{2}\{-(n_r^2-n_i^2-\cos^2\tau)\\ &\qquad+[(n_r^2-n_i^2-\cos^2\tau)^2+4n_r^2n_i^2]^{\frac{1}{2}}\}\end{aligned}\right\}. \tag{7}$$

b. Diffraction

The angular gain for diffraction by a single sphere is given by van de Hulst (1957) as

$$G_1^F(\theta,x)=G_2^F(\theta,x)=2x^2\left[\frac{J_1(x\sin\theta)}{x\sin\theta}\right]^2, \tag{8}$$

where J_1 is the Bessel function of the first kind. The diffraction depends on the particle size parameter but is independent of the index of refraction.

c. Integration over particle size

The ray-optics results for single scattering by a polydispersion of spherical particles is obtained by integrating over the given particle size distribution $n(x)$, where $n(x)dx$ is the number of particles per unit volume with size parameter between x and $x+dx$. Since in ray optics each particle scatters an amount of energy in proportion to x^2, the gain for a polydispersion is given by

$$G_{1,2}(\theta)=\frac{\int_{x_1}^{x_2}G_{1,2}(\theta,x)x^2n(x)dx}{\int_{x_1}^{x_2}x^2n(x)dx}. \tag{9}$$

This integration over particle sizes has no effect on the geometrical-optics results except in the case where there is absorption. The primary effect of the integration is to average out the maxima and minima in the diffracted light. Hence, it may often be sufficient to make ray-optics calculations for an appropriate mean particle size $\bar{x}$, and omit the integration over sizes. We have made the integration (9) only to allow the fairest comparison of the ray-optics approximation to Mie scattering with the same size distribution.

The size distribution we employ is the gamma function used previously by Deirmendjian (1964) and Hansen and Pollack (1970), i.e.,

$$n(x)\propto x^6e^{-6x/x_m}. \tag{10}$$

The distribution has its mode at $x=x_m$ which in this paper was given the values 25, 100 and 400. The integration limits used were $x_1=0$ and $x_2=800$.

3. Mie scattering

Mie scattering theory (described, e.g., by van de Hulst, 1957) gives the exact intensity and polarization for scattering by finite homogeneous isotropic spheres for an incident plane wave in an arbitrary state of polarization. The results for a single particle may be described, using the notation of van de Hulst, by four functions of the scattering angle:

$$\left.\begin{aligned} M_1(\theta)&=|A_1(\theta)|^2,\\ M_2(\theta)&=|A_2(\theta)|^2,\\ S_{21}(\theta)&=|A_2(\theta)A_1^*(\theta)+A_1(\theta)A_2^*(\theta)|/2,\\ D_{21}(\theta)&=i|A_2(\theta)A_1^*(\theta)-A_1(\theta)A_2^*(\theta)|/2\end{aligned}\right\}, \tag{11}$$

where A_1 and A_2 are complex scattering amplitudes (van de Hulst), respectively parallel and perpendicular to the scattering plane; i is $(-1)^{\frac{1}{2}}$; and the asterisk indicates the complex conjugate. For a size distribution (polydispersion) of independent scatterers the functions M_1, M_2, S_{21} and D_{21} are obtained by simply adding those functions (M_1, etc.) for all particles in the distribution.

Let $\mathbf{P}$ be the phase matrix defined with respect to the Stokes parameters I, Q, U and V; $\mathbf{P}$ has four rows and four columns, with P^{ij} representing the element in the ith row and jth column. The non-zero elements for Mie scattering are given by

$$\left.\begin{aligned} P^{11}(\theta)&=P^{22}(\theta)=C[M_1(\theta)+M_2(\theta)]/2\\ P^{12}(\theta)&=P^{21}(\theta)=C[M_2(\theta)-M_1(\theta)]/2\\ P^{33}(\theta)&=P^{44}(\theta)=CS_{21}(\theta)\\ P^{43}(\theta)&=-P^{34}(\theta)=CD_{21}(\theta)\end{aligned}\right\}, \tag{12}$$

where M_1, M_2, S_{21} and D_{21} refer to either a single particle or a polydispersion, as the case may be; $P^{11}(\theta)$ is the phase function; and the constant C in (12) is

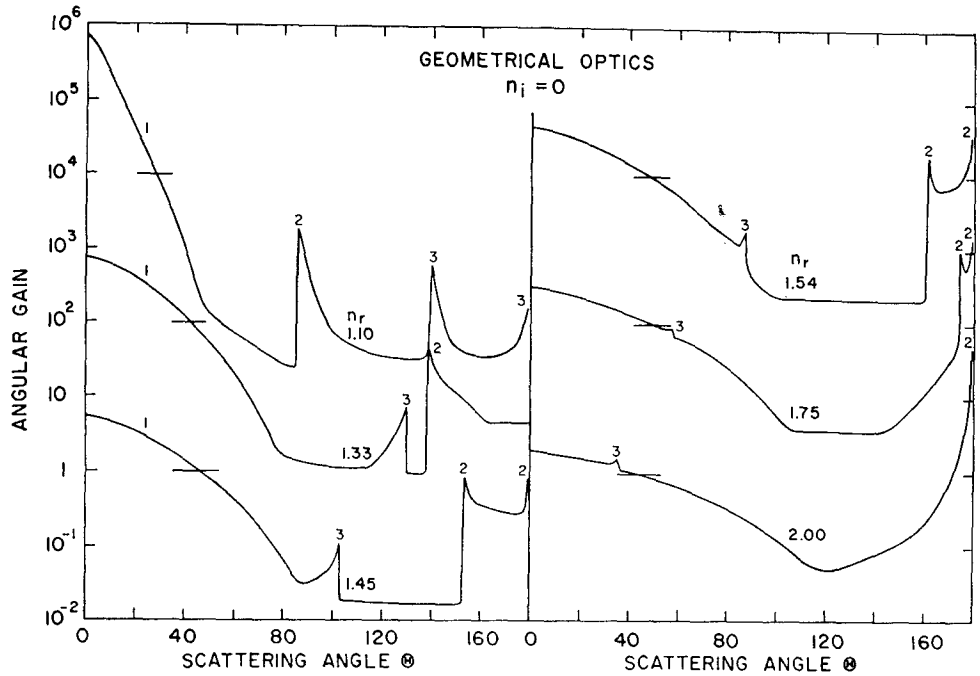

FIG. 1. Angular gain for geometrical optics for incident unpolarized light including as many as two internal reflections, $\sum_{p=0}^{3}[G_1^{(p)}+G_2^{(p)}]/2$. The small numbers on strong features represent the value of p contributing most to each feature. The vertical scale applies to the lowermost curves ($n_r=1.45$ and 2.00). The other curves are successively displaced upward by factors of 10^2, with the horizontal bars occurring where the gain is unity.

defined such that P^{11} is normalized as

$$\frac{1}{4\pi}\int_{4\pi} P^{11}(\theta)d\omega = 1. \tag{13}$$

In view of the above definitions we compared P^{11} from Mie theory to $(G_1+G_2)/2\bar{\omega}_0$. We also compared P^{12}/P^{11} to $(G_2-G_1)/(G_1+G_2)$; these are labeled "degree of polarization" in the figures.

For the ray-optics results to be useful in multiple scattering theory it is also important to obtain approximations for P^{33} and P^{43}. However, Hansen (1971) has shown that the element CD_{21} often has a negligible effect on the multiple scattering. This is a result of the fact that CD_{21}, and hence also the phase difference between the scattered intensities in the directions perpendicular and parallel to the scattering plane, are small at most scattering angles. We therefore propose that the ray-optics approach described in this paper may often be used with a sufficient accuracy by assuming that $P^{43}=0=P^{34}$, and that P^{33} is approximated by $(G_1G_2)^{\frac{1}{2}}$. A partial test of this is obtained below.

TABLE 1. Scattering angles for the first four components of geometrical optics.

n_r	External reflection ($p=0$)	Two refractions ($p=1$)	One internal reflection ($p=2$)	Two internal reflections ($p=3$)
1.10	0–180°	0–49°	85–180°	0–180°
1.33	0–180°	0–82°	138–180°	0–129°
1.45	0–180°	0–93°	153–180°	0–102°
1.54	0–180°	0–99°	161–180°	0–86°
1.75	0–180°	0–110°	140–180°	0–57°
2.00	0–180°	0–120°	121–180°	0–35°

4. Numerical results

The calculations for geometrical optics were made with 181 equally spaced incident directions, i.e., for intervals of 0.5° in τ. The scattered intensities were obtained separately for each of the first four components, $p=0$, 1, 2 and 3, at the resulting scattering angles. Linear interpolation was then used on each component to obtain results at each degree of scattering angle in the range 0–180°. For each of the refractive indices considered, the energy contained in the neglected components was $<1\%$ of the total scattered energy.

a. Geometrical optics

Fig. 1 illustrates the average gain for the two polarization components for geometrical optics. This is proportional to the single-scattered intensity for incident unpolarized light. Results are shown for six refractive indices in the range $n_r=1.1$–2.0; the indices include 1.33, which is approximately valid for water at most wavelengths from the visual to the near infrared; 1.45, which has been deduced for the refractive index

TABLE 2. Incident (τ) and scattering (θ) angles for the glory and rainbows.

	Glory for $p=2$		Rainbow for $p=2$		Rainbow for $p=3$		Rainbow for $p=4$		Rainbow for $p=5$		Rainbow for $p=6$	
n_r	τ	θ	τ	θ	τ	θ	τ	θ	τ	θ	τ	θ
1.10	—	—	15°	84°	9°	139°	7°	170°	5°	119°	4°	71°
1.33	—	—	30°	137°	18°	130°	13°	43°	10°	42°	9°	123°
1.45	3°	180°	37°	152°	22°	102°	16°	4°	12°	92°	10°	178°
1.50	7°	180°	40°	157°	23°	93°	17°	9°	13°	109°	11°	158°
1.54	11°	180°	43°	161°	24°	86°	18°	19°	14°	121°	11°	142°
1.75	30°	180°	56°	173°	31°	58°	22°	60°	17°	175°	14°	78°
2.00	57°	180°	90°	180°	38°	35°	27°	94°	21°	140°	17°	24°

of the Venus cloud particles at visual wavelengths (Hansen and Arking, 1971; Hansen and Hovenier, 1971); and 1.54, which is sometimes used for terrestrial aerosols. The small numerals on the strong features in the gain indicate the value of p contributing most to the feature.

The contribution to the scattered light from $p=0$ (external reflection) does not leave any apparent feature on the gain for the case of no absorption ($n_i=0$) with $1.1\leqslant n_r\leqslant 2.0$. This is partly a result of the fact that the amount of energy in $p=0$ is a relatively small percent of that in all components; for the refractive indices considered, it is greatest at $n_r=2.0$ where it is $\sim 15\%$. Also the reflected energy is distributed smoothly over the entire range $0\leqslant\theta\leqslant 180°$, increasing to a maximum at $\theta=0°$ where the energy in $p=1$ is greater.

Most of the scattered energy is contained in the $p=1$ component (twice refracted rays), increasing from $\sim 73\%$ at $n_r=2.0$ to $\sim 95\%$ at $n_r=1.1$. The energy for $p=1$ is concentrated in the forward direction (see column 3 of Table 1 and Fig. 1), increasingly so for decreasing n_r. This component, along with diffraction (Section 4b) and $p=0$ in the case of large n_r or n_i, primarily determines the value for the asymmetry of the phase function (Hansen and Pollack, 1970), which is a basic parameter in radiative transfer.

The components involving one or more internal reflections ($p\geqslant 2$) contain $\lesssim 11\%$ of the scattered energy for $n_r\leqslant 2$ with $n_i=0$, and this percentage decreases to zero as n_i increases. However, these rays can give rise to easily observable optical phenomena, the glory and rainbows, which are very useful for cloud particle identification (Hansen, 1971).

Rainbows occur when the scattering angle θ has an extremum as a function of the angle of incidence τ on the sphere. For $n_r=1.33$, as τ is varied from 90° (central incidence) to 0°, the scattering angle for rays internally reflected once ($p=2$), computed using Snell's law, decreases from 180° until it reaches $\sim 137.5°$ (the angle of "minimum deviation") where it then increases again. The resulting concentration of energy at 137.5° and just greater angles is the "primary rainbow." Similarly, the $p=3$ rays for $n_r=1.33$ have an angle of "maximum deviation" at 129.9°, corresponding to the "second rainbow" for water drops. As indicated by van de Hulst (1957), the location of the rainbows can generally be obtained from the condition $d\theta/d\tau=0$, which yields

$$\sin\tau=[(n_r^2-1)/(p^2-1)]^{\frac{1}{2}}. \tag{14}$$

Table 2 gives the corresponding scattering angles for the first five rainbows for several values of $1.1\leqslant n_r\leqslant 2.0$. Fig. 1 also illustrates how the rainbows move as the refractive index is varied. In this figure the sharp peaks at angles other than 0° or 180° are all rainbows for $p=2$ or $p=3$. In each rainbow, according to geometrical optics, the peak in the intensity or gain extends to infinity; in the figures, however, the peaks are finite because the calculations are made only at integral degrees of the scattering angle.

Infinite intensities, as indicated in Section 2a, can occur in one case other than the rainbows, namely in the glory at $\theta=180°$ and the comparable phenomena at $\theta=0°$. The condition for having a glory for the $p=2$ rays is that the refractive index be between $2\frac{1}{2}$ and 2. For $n_r=2$ the glory and rainbow, both for $p=2$, coincide at $\theta=180°$ giving rise to greatly enhanced backscattering (Fig. 1), as previously found from Mie theory by Hansen and Pollack (1970). The glory shown for $n_r=1.1$ is due to $p=3$ with the incident angle $\tau\approx 35°$. For all other refractive indices shown in Fig. 1, except $n_r=1.33$, there is an infinite intensity at $\theta=180°$ caused by the glory for $p=2$. There is, however, no comparable phenomena at $\theta=0°$ for the refractive indices and components considered ($p\leqslant 3$).

For $n_r=1.33$, as discussed by van de Hulst, there is no glory in geometrical optics for $p\leqslant 4$, and the higher components contain a negligible amount of energy. The fact that a glory is observed in nature for water drops points out one of the greatest discrepancies between ray optics and Mie theory (see Section 4b). For finite particles there is a contribution to the backscattering from edge rays ($\tau\approx 0°$), apparently connected with surface waves generated on the sphere (Bryant and Cox, 1966; Fahlen and Bryant, 1968; van de Hulst, 1957). However, a satisfactory mathematical description of the glory, other than that hidden in the complete Mie formalism, is still lacking.

Fig. 2 shows the degree of linear polarization computed from geometrical optics. Unlike the case for the gain (Fig. 1), the external reflection ($p=0$) has a strong influence on the polarization. This is partly because the external reflection is strongly polarized; e.g., for

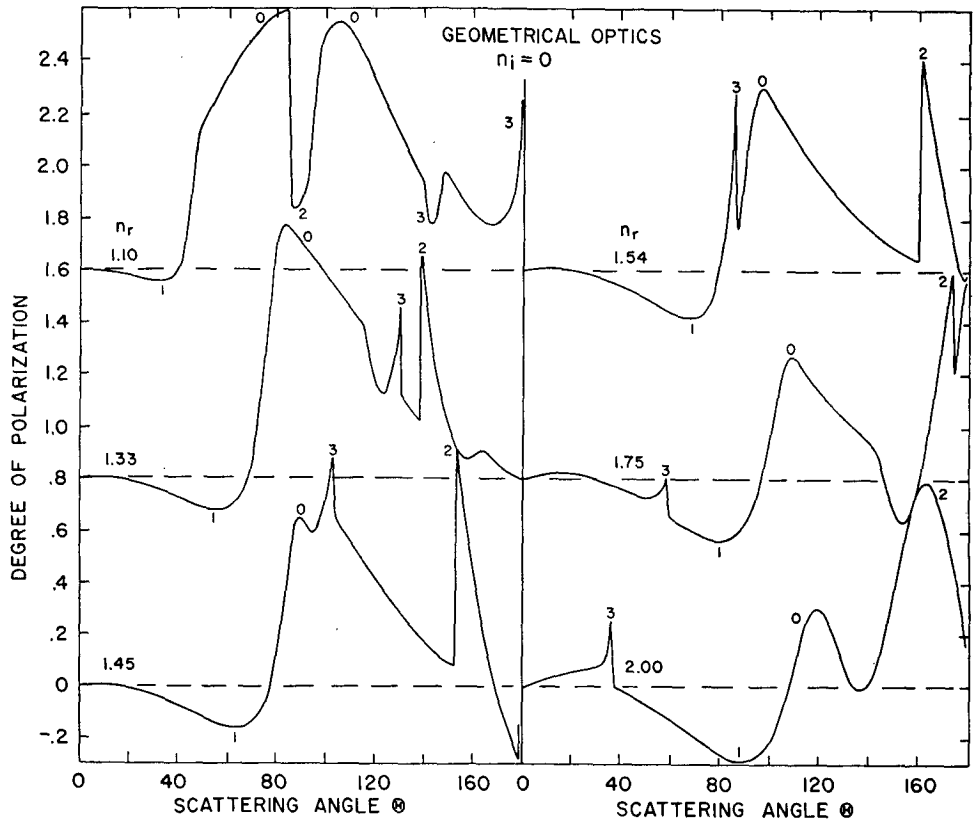

FIG. 2. Degree of linear polarization for geometrical optics for incident unpolarized light, $\sum_{p=0}^{3}\{[G_2^{(p)}-G_1^{(p)}]/[G_1^{(p)}+G_2^{(p)}]\}$. The small numbers on strong features represent the value of p contributing most to each feature. The vertical scale applies to the lowermost curves. The other curves are successively displaced upward by 0.8, with the zero points of the polarization indicated by dashed lines.

the refractive indices 1.33, 1.54 and 1.75, the external reflection alone has a maximum polarization of 97, 71 and 48% at scattering angles of 82, 97 and 108°, respectively. It is also partly due to the fact that at angles where the polarization for $p=0$ is strong, the intensity for the higher components ($p \geq 1$) is small. For some refractive indices, e.g., $n_r=1.1$ and 2.0, features due to different components overlap causing unusual polarization patterns. The polarization should, of course, be studied in conjunction with the gain; as an example, the negative polarization associated with $p=1$, though it does not appear particularly prominent in Fig. 2, can be very important because of the large amount of energy in that component.

b. Comparison of ray optics and Mie theory

Mie scattering computations were made for comparison to ray optics for two refractive indices, $n_r=1.33$ and 1.50. The particle size distribution was that given by (10) with x_m equal to 25, 100 and 400. The Mie calculations were made at 245 scattering angles, 0(0.1) 2(0.25)5(0.5)10(1)170(0.5)175(0.25)178(0.1)180°. The integration over particle size was made from $x_1=0$ to $x_2=800$.

Fig. 3 compares phase functions from Mie theory to the corresponding results for ray optics. The phase functions for each size parameter are successively displaced by two orders of magnitude to allow a clear comparison. There are thus three curves for ray optics even though they differ from each other only in their Fraunhofer diffraction peaks. From these comparisons we note the following.

There is close agreement between ray optics and Mie theory when the size parameter is as large as 400. An exception is the glory for $n_r=1.33$ which, as discussed above, does not occur in the ray-optics results. Otherwise, most of the discrepancies and their variation with the size parameter can be qualitatively well understood in terms of the increasing inapplicability of the localization principle for decreasing size parameters. This causes the light in the individual features to be blurred over a wider range of angles than predicted by ray optics. This affects higher values of p first because they have a more detailed ray path within the particle. Thus, the secondary rainbow ($p=3$) is quite smooth at $x_m=100$, and is lost at $x_m=25$, while the primary rainbow ($p=2$) is still easily visible. The number of rainbows visible in the intensity thus gives some indica-

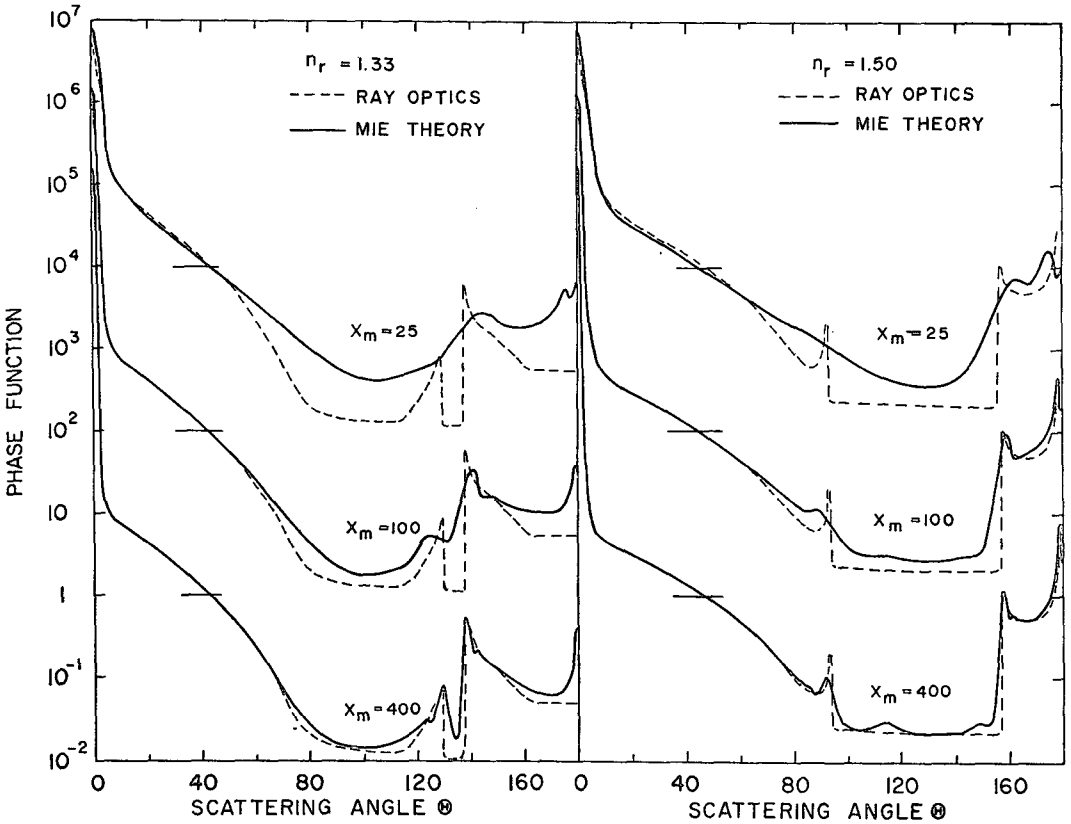

FIG. 3. Comparison of ray optics and Mie theory for phase functions. Two refractive indices are shown and three size distributions [Eq. (10)]. The vertical scale applies to the lowermost curves ($x_m=400$). The other curves are successively displaced upward by factors of 10^2, with the horizontal bars occurring where the phase function has the value unity.

tion of the particle size, but the polarization, discussed below, provides a much more precise means for particle sizing.

The rainbows, in addition to being smoothed out, tend to move away from their ray-optics locations as the size parameter decreases. This is apparently just another manifestation of the spreading out of rays for finite size parameters; indeed, simply applying a smoothing function to the ray-optics rainbows would cause the peaks to move in the observed senses, due to the asymmetry of the rainbows. Note also that regions where the intensity is very low for ray optics, e.g., $\theta\approx 90°$ for $n_r=1.33$ and $\theta\approx 130°$ for $n_r=1.50$, tend to be filled in for smaller particles. However, the region of twice-refracted light is approximated well by ray optics even for x_m as small as 25, because it arises from a small value of p *and* does not involve a sharp feature.

Finally, we note the following minor features in Fig. 3. For Mie scattering with $x_m=400$, the small secondary peaks on the less steep side of the rainbows are supernumerary bows. These are interference phenomena and hence are not rendered by ray optics in which the phase is neglected. There is also a small but noticeable discrepancy in the diffraction peak. The higher value for Mie scattering may perhaps arise from surface waves which scatter in the forward direction. For $n_r=1.50$ and $x_m=400$ the feature at $\theta\approx 115°$ is probably the rainbow for $p=5$.

Fig. 4 compares the degree of linear polarization for ray optics and Mie theory. The polarization for ray optics is illustrated only in the case $x_m=400$; the results for the other size parameters do not differ significantly from that case. As was the case for intensities, ray optics and Mie theory are in rather good agreement for $x_m=400$, but the discrepancies increase rapidly for smaller size parameters.

The polarization, compared to the intensity, contains much stronger imprints of most of the features occurring in the scattered light, as illustrated by Figs. 3 and 4. Furthermore, for the polarization these features remain visible to much smaller size parameters. These conclusions hold for the rainbows, the supernumerary bows, the glory, and the external reflection. The strength of these features under single scattering is a major reason why there is a high information content in polarization observations. The importance of polarization as compared to intensity is further heightened by the fact that there is much less tendency for multiple scattering to wash out such features in the polarization results (Hansen, 1971).

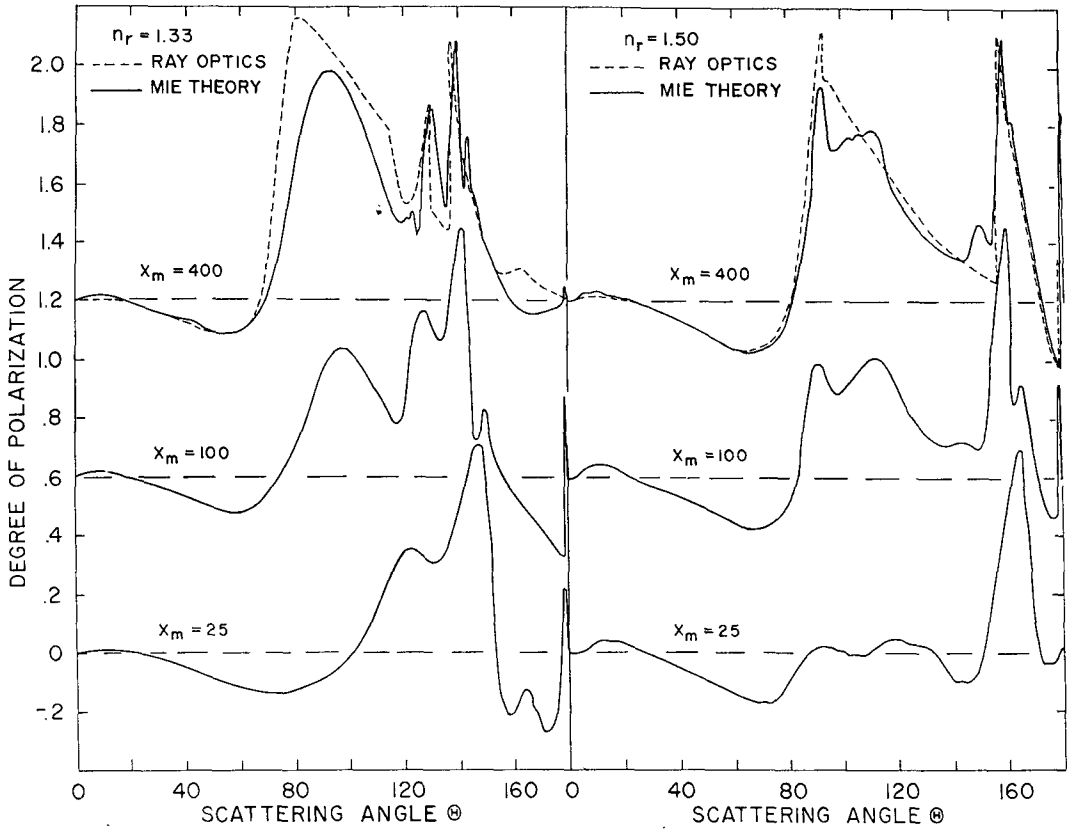

FIG. 4. Comparison of ray optics and Mie theory for the degree of linear polarization. Two refractive indices are shown and three size distributions [Eq. (10)]. The vertical scale applies to the lowermost curves ($x_m = 25$). The other curves are successively displaced upward by 0.6, with the zero points of the polarization indicated by dashed lines. The border is broken at $\theta = 180°$ so that the glory may be illustrated.

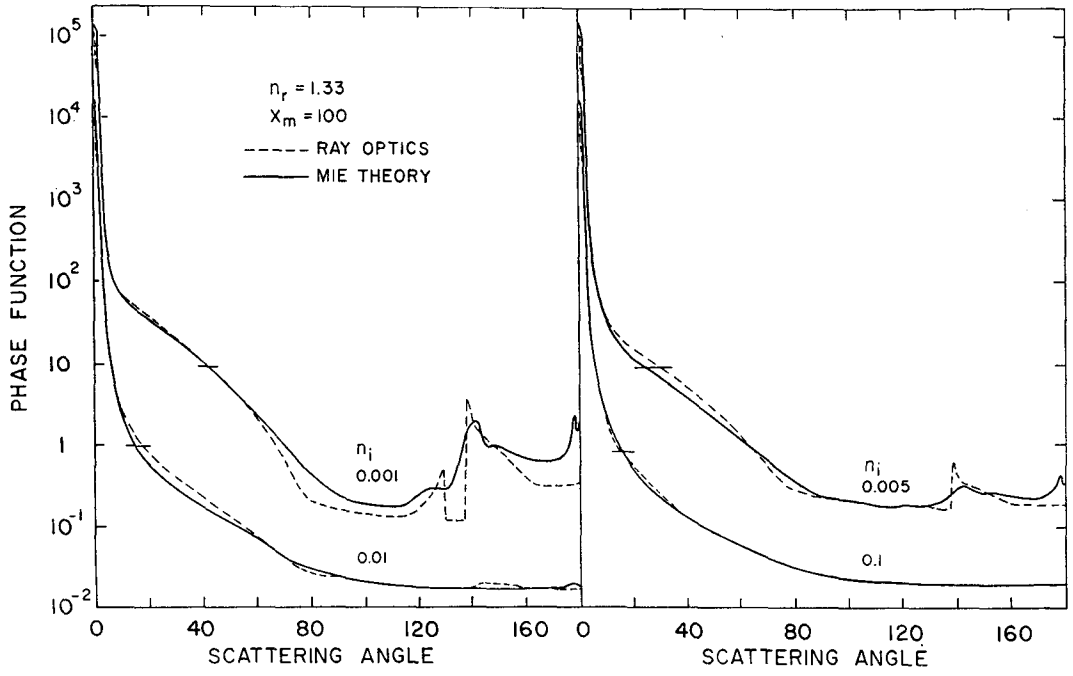

FIG. 5. Comparison of ray optics and Mie theory for the phase function in cases for which the absorption within the particles is significant. All curves are for a real refractive index $n_r = 1.33$ and a mode size parameter $x_m = 100$. The vertical scale applies to the lowermost curves ($n_i = 0.01$ and 0.1). The other two curves are displaced upward by a factor 10.

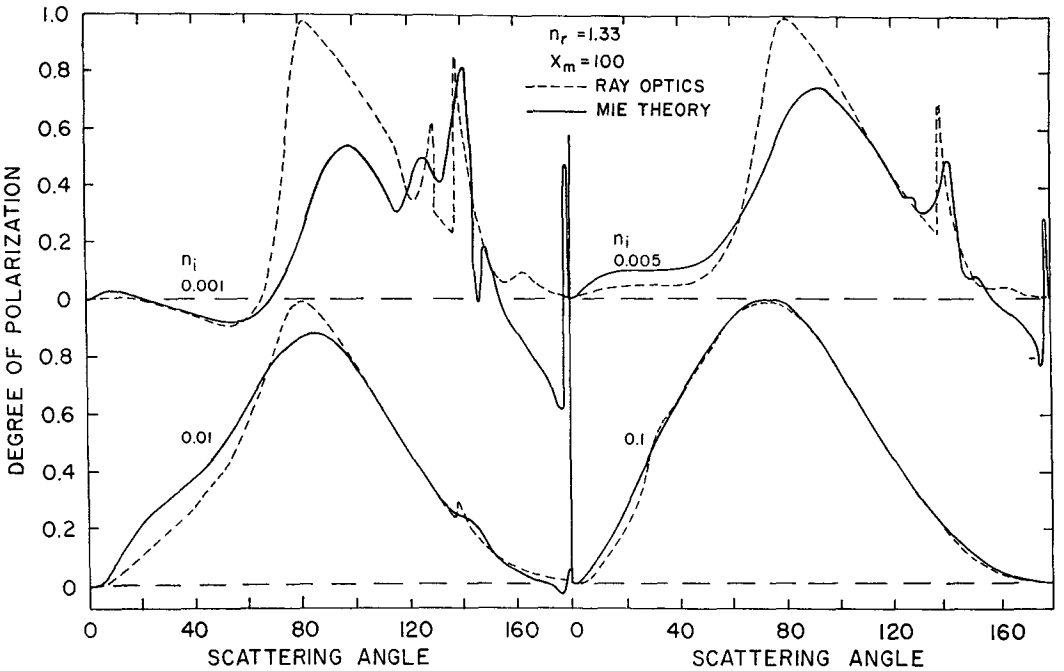

FIG. 6. Comparison of ray optics and Mie theory for the degree of linear polarization in cases for which the absorption within the particles is significant. All curves are for a real refractive index $n_r=1.33$ and a mode size parameter $x_m=100$.

While most of the features in Fig. 4 can be understood on the basis of our discussion of Fig. 3, the following additional comments may be useful. For $n_r=1.50$ both $p=0$ and $p=3$ contribute significantly to the polarization for $\theta\approx 90°$. The feature at $\theta\approx 120°$ for $n_r=1.33$ and $x_m=25$ is primarily due to the $p=3$ rainbow. For $x_m=100$ the first supernumerary bow of the primary rainbow is easily visible for both $n_r=1.33$ and 1.50. For $\theta\approx 10$–$20°$ Mie theory gives a higher polarization than ray optics.

Figs. 5 and 6 illustrate how absorption ($n_i\neq 0$) affects the comparison of ray optics and Mie theory. As could be anticipated the comparison improves considerably as n_i increases. Thus, most of our comparisons have been made in the extreme for which ray optics is least accurate ($n_i=0$); however, in terrestrial and other planetary applications n_i is commonly negligible. The reason that the comparison improves with increasing n_i is that the absorption cuts out the highest components (largest p) first; these components are the least accurately rendered by ray optics because they have a complicated ray path and because they include the rainbows and glory. Increasing n_i also increases the contribution of external reflection which should be the component most appropriate for application of geometrical optics.

If the ray-optics solution is to be used in multiple scattering theory, it is necessary, in principle, to know the entire phase matrix. Therefore, in Fig. 7 we compare P^{33} computed from Mie theory to $(G_1G_2)^{\frac{1}{2}}$ computed from ray optics; the comparison is for the case $n_r=1.33$ with $x_m=100$. The two curves are almost identical for scattering angles $\lesssim 70°$, where most of the photons are scattered. In the same region P^{43} is much smaller than P^{33}. Hansen (1971) has found that for scattering of sunlight (unpolarized) by water clouds the error introduced by neglecting P^{43} (i.e., setting $P^{43}=0=P^{34}$) usually has a negligible effect on the in-

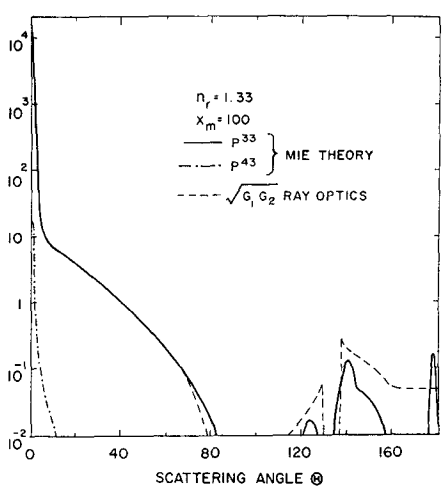

FIG. 7. Comparison of ray optics and Mie theory for a real refractive index $n_r=1.33$, a mode size parameter $x_m=100$, and no absorption ($n_i=0$). The two curves from the Mie calculations are the matrix elements P^{33} and P^{43}. The curve for ray optics is $(G_1G_2)^{\frac{1}{2}}$ which approximates P^{33} where P^{33} has a large value. For $\theta\gtrsim 70°$, $|P^{43}|$ is of comparable magnitude to P^{33}; however, negative values of P^{43} are not included in this figure.

tensity and degree of polarization in multiple scattering. Therefore, we believe that the ray-optics approach described in this paper can often be used as a good approximation for the entire phase matrix for a polydispersion of spherical particles. We have, however, not yet tested this by using a ray-optics phase matrix in a multiple scattering program.

5. Discussion

The computations illustrated in this paper are useful for establishing how reliable ray-optics calculations are for different particle size parameters. The accuracy required depends, of course, on the intended application, but the agreement between ray optics and the exact Mie theory is quantitatively quite good for size parameters of the order of 400. For smaller size parameters, the comparison of ray optics to Mie theory for different size parameters provides some understanding of several features which occur in Mie theory, and of the dependence of these features on refractive index and particle size parameter.

For many shapes of non-spherical particles it will be very difficult to obtain an exact solution for single scattering, comparable to the Mie solution for spheres. However, ray optics may provide a more tractable approach. The computations that we have made for spheres are therefore useful as a quantitative test of the ray-optics approach in a case for which an exact solution is available. The light scattered by non-spherical particles is also divided among the various components, $p=0$ (external reflection), $p=1$, etc., and hence the validity of ray-optics calculations, once they are obtained, can be estimated based on these comparisons for spheres and on the geometry involved in causing the given features for non-spherical particles. For example, particles in terrestrial ice clouds usually have a mean radius $\gtrsim 20\,\mu$; hence, ray-optics computations such as those by Jacobowitz (1970) for hexagonal cylinders can potentially yield an accurate description of the scattering at visual wavelengths. On the other hand, O'Leary's (1970) claim that particles 1–$4\,\mu$ in radius can produce a halo a few degrees in width in the visual and infrared at the scattering angle predicted by ray optics is extremely doubtful.

Acknowledgments. We would like to thank J. W. Hovenier and R. M. Schotland for discussions and Dr. Robert Jastrow for his hospitality at the Institute for Space Studies. The authors are pleased to acknowledge assistance involving a National Research Council Postdoctoral Research Associateship supported by NASA (K. L.) and NASA Grant 33-008-012 through Columbia University (J. E. H.).

REFERENCES

Born, M., and E. Wolf, 1964: *Principles of Optics*. New York, Macmillan, 808 pp.

Bryant, H. C., and A. J. Cox, 1966: Mie theory and the glory. *J. Opt. Soc. Amer.*, **56**, 1527–1532.

Deirmendjian, D., 1964: Scattering and polarization properties of water clouds and hazes in the visible and infrared. *Appl. Opt.*, **3**, 187–196.

Fahlen, T. S., and H. C. Bryant, 1968: Optical backscattering from single water droplets. *J. Opt. Soc. Amer.*, **58**, 304–310.

Hansen, J. E., 1971: Multiple scattering of polarized light in planetary atmospheres. Part II. Sunlight reflected by terrestrial water clouds. *J. Atmos. Sci.* (in press)

——, and A. Arking, 1971: Clouds of Venus: Evidence for their nature. *Science*, **171**, 669–672.

——, and J. W. Hovenier, 1971: Properties of the visible clouds of Venus. Presented at February 1971 meeting, Amer. Astron. Soc., Tallahasee, Fla (paper in preparation).

——, and J. B. Pollack, 1970: Near infrared light scattering by terrestrial clouds. *J. Atmos. Sci.*, **27**, 265–281.

Hodkinson, J. R., and I. Greenleaves, 1963: Computations of light-scattering and extinction by spheres according to diffraction and geometrical optics, and some comparisons with the Mie theory. *J. Opt. Soc. Amer.*, **53**, 577–588.

Jacobowitz, H., 1970: Emission, scattering and absorption of radiation in cirrus cloud layers. Ph.D. thesis, Dept. of Meteorology, M.I.T.

O'Leary, B., 1970: Venus halo: Photometric evidence for ice in the Venus clouds. *Icarus*, **13**, 292–298.

Shifrin, K. S., 1951: Scattering of light in a turbid medium. NASA TT F-477, 212 pp (1968 translation of Russian edition).

——, and Yu. I. Rabinovich, 1957: The spectral indicatrices of large water drops and the spectral polarization of rainbows. *Bull. Acad. Sci., USSR, Ser. Geophys.*, **12**, 73–89.

van de Hulst, H. C., 1957: *Light Scattering by Small Particles*. New York, Wiley, 470 pp.

Volz, F., 1961: Der regenbagen. *Handbuch der Geophysik*, Vol. 8, Berlin, Borntraeger 943–970.